Proc. Estonian Acad. Sci. Eng., 2007, **13**, 4, 384–393

A new instrument for remote sensing of thermal anomalies, based on minimal thermal change detection

Volker Tank

German Aerospace Centre, Remote Sensing Technology Institute, Oberpfaffenhofen, D-82234 Wessling, Germany; Volker.Tank@dlr.de

Received 17 July 2007

Abstract. Thermal anomalies are phenomena of unexpected thermal behaviour, caused by thermal effects unknown in the first instance. In land and water bodies these may origin, for example, from gases emerging from deep reservoirs or from springs, submerged in water bodies. Their surface thermal impact is superimposed to the environmental thermal impact and dampens the changes induced by the latter. The method of minimal thermal change detection utilizes this effect to identify and investigate such events. It applies repeated acquisition of congruent infrared images of areas of interest under changing thermal environment. From these images, regions of low thermal change are identified. Application to natural CO_2 vents resulted in their reliable localization. Tools for the measurement of vent gas flux and temperatures were developed and successfully applied.

Key words: thermal anomalies, gas vents, gas flux.

1. INTRODUCTION

This work was stimulated by the demand to identify vents of CO_2 on the earth surface and to determine their gas flux and the gas areal reach originating from two scientific tasks.

1. Continuous increase of atmospheric CO_2 has stimulated an intensive research on the global atmospheric carbon budget which so far has been dominated by biological, volcanic and anthropogenic fluxes, being considered as the main contributors. The scope has been widened in a recent survey through the inclusion of lithospheric, non-volcanic carbon degassing,

contributing about 10^2 to 10^3 Mt CO_2 per year [1]. It is suggested to assess CO_2 and also CH_4 fluxes through new field measurements.

2. During the last decades an intensive research has been performed also on physiological reactions of plants under high CO_2 environments. Among various approaches, investigations on CO_2-rich locations (i.e., emissions occurring in vents or mofettes), have been selected as specifically attractive introducing a minimum of experimental intervention to these "natural laboratories". However, since the environment of such sites is beyond the investigator's control, determination of influential parameters is required, among which monitoring the small scale CO_2 concentration is of prime importance [2–4].

Current investigation techniques employ gas collection instrumentation, resulting in laborious data collection if larger vent areas are to be investigated [5], and hence are not appropriate for large-scale or non-interfering monitoring. An efficient solution of the problem is the method of minimal thermal change detection [6]. Its application to the investigation of other thermal anomalies besides CO_2-vents seems also promising.

2. METHODOLOGY

2.1. Principle

The surfaces of congeneric land bodies and also of common water bodies can be expected to adopt almost identical temperatures when exposed to environmental influences such as sun, wind and weather in an identical way. This is the case when air temperature, wind velocity, sun illumination, etc. influence each surface element in the same way. Such conditions take place in moderate size body areas of the same elevation, orientation to sun and surface constitution. Furthermore, the thermal characteristics like heat capacity and thermal conductivity of the body and its underground must be alike everywhere as well as the heat exchange taking place through radiation, conduction and convection. Identical changes of thermal impact will then result in identical surface thermal response. This is true for a macroscopic view, which averages small-scale thermal inhomogeneities caused, for example, by mechanical surface structures. Any additional thermal impact, confined to a limited area of such bodies, will modify the adopted thermal characteristics of this confined area. That is commonly called a thermal anomaly. Being superimposed to all natural thermal influence variations and temporal cycles (day and night, sun and clouds, etc.) the confined thermal impact will dampen the thermal response of the object's confined area to these variations and cycles. It is assumed that for the time interval of observation the confined impact is stable in comparison to the variations of the natural influence. Then temperature variations appear to be less at the confined impact area than at the rest of the body surface, resulting in a zone of minimal thermal change within the congeneric region. This effect is

utilized with the method of minimal thermal change detection by identifying these zones within thermal image time series data sets, taken at different times and under different environmental conditions.

2.2. Instrumentation

To access thermal images of the test area an AGEMA 570 camera was used. Technical parameters of the camera are listed in Table 1.

The spectral sensitivity of the camera covers wavelengths from 7.5 to 13 μm, a region of very weak radiative activity of gaseous CO_2. Hence no direct infrared signature of CO_2 can be expected to be acquired with the system. According to the Planck law of radiation, however, the band from 7.5 to 13 μm wavelength resembles the spectral region of highest radiative flux of objects at ambient temperatures (around 20 °C). It is therefore best suited to detect thermal changes of surfaces at ambient temperatures. The camera is interfaced to a laptop computer providing remote camera control and data acquisition and storage at selectable frame rates as fast as 1 Hz.

The camera system display provides temperature-scaled scene images. For this the system software calculates the "radiance temperature" by assuming the scene to be a black body (defined as emissivity unity). Natural and most artificial objects are not black bodies, their emissivity is smaller than unity. There is the provision to input emissivity values of the surfaces in the scene if these are known in order to determine the scene temperatures more accurately. The method of thermal change detection is based on temperature relations, hence it is considered sufficient to get precise relative temperatures in the scene; high accuracy of the true temperatures is not required. Therefore emissivity values have not been introduced. The situation is different with the calculation of gas flux as will be explained later.

Table 1. Parameters of the thermovision system

Camera type	AGEMA ThermoVision 570
Principle	Uncooled microbolometer focal plane array
Detector	Vanadiumoxide 320 × 240 elements
Spectral range	7.5–13 μm
Field of view, FOV	12° × 9°, alternative 24° × 18°
Spatial resolution	0.65 mrad, resp. 1.3 mrad resembling: 3.1 cm in 48 m, resp. 6.2 cm in 48 m distance
Temperature resolution	0.15 K @ 300 K
Image frequency	50 Hz

2.3. Minimal thermal change detection

Application of the minimal thermal change detection procedure requires the acquisition of a time series of two or more geometrically congruent thermal images of the area of investigation, taken at different ambient thermal conditions. Within such datasets or subsets for every picture element (pixel) the maximum and minimum temperature are identified and their difference is calculated. These pixels are collected in a single image frame of maximum temperature differences. The pixels of least difference (minimal thermal change) are suspect to thermal anomaly. Careful investigation of the image area with respect to the degree of its congeneric constitution and the quantification of the anomaly is required to find the presence of a confined thermal impact. Without *a priori* knowledge, the nature of such an impact must be revealed by field inspection. For regions known for containing anomalies like gas vent fields, investigated for this work, the comparison of the surface temperature of congeneric objects within and out of thermal reach of the detected anomaly is in general a sufficiently reliable proof of the presence of a confined thermal anomaly.

2.4. Determination of the quantity of the emitted gas

For vents of CO_2, the comparison of the surface temperature of congeneric objects within and out of thermal reach of the anomaly is the basis for the determination of gas quantities emitted. The method developed aims at the quantification of the heat energy Q, necessary to generate the observed thermal anomaly.

The time series of the surface temperature distribution collected resembles a record of the result of elapsed heat energy transfer processes inside and among the scene constituents for every picture pixel (object element oxel). Applying the method, two classes of pixels/oxels will be distinguished: those belonging to the anomaly (within the thermal reach of the gas) and those being normal (out of thermal reach of the gas). Total heat energy transfer consists of conductive, convective and radiation fluxes.

Radiation flux can be calculated from the temperature and emissivity of the object applying the Kirchhoff and Stefan–Boltzmann laws

$$E_a = \varepsilon \sigma T_a^4, \tag{1}$$

$$E_n = \varepsilon \sigma T_n^4, \tag{2}$$

where E is radiation flux [W/cm^2], ε is emissivity of the object, σ is 5.67×10^{-12} [W/(cm^2 K^4)], T is temperature of the object [K], a is the index referring to oxels of thermal anomaly and n is the index referring to "normal" oxels (no thermal anomaly).

Equations (1) and (2) resemble an approximation, valid for large emissivity, prevailing in most natural materials in the considered spectral region. Low

emissivity would require reflected and eventually transmitted radiation to be taken into account.

The heat energy Q_R, emitted through radiation flux, is calculated as the integral of the flux E over the radiating area A and time t

$$Q_R = \int_t \int_A E \, \mathrm{d}A \mathrm{d}t. \tag{3}$$

The difference ΔQ_R between the heat energy, emitted by the anomaly oxels and the heat energy, emitted by normal oxels is

$$\Delta Q_R = \int_t \int_A | E_n - E_a | \, \mathrm{d}A \mathrm{d}t. \tag{4}$$

Convective flux is neglected during the time of observation (evening, night and early morning). This is justified by observed accumulation of gas in the doline over night.

Conductive flux takes place inside the materials of the scene (air, travertine rubble, reed, etc.). With reference to the principle of minimal thermal change detection, only conduction between gas and surfaces within thermal reach of the gas needs to be included. All other conductive fluxes contribute to the observed effects in the same manner and are considered to cancel out.

Hence, in a first approximation it is assumed that the heat energy, causing the thermal anomaly, is provided (or absorbed) solely by the gas through conduction in the boundary layer between gas and surface. During this process the gas undergoes a temperature change ΔT_G, defined as the difference between the exit temperature T_{Ge} of the vent gas and the vent gas temperature T_{Gf}, acquired after finalization of the energy exchange between gas and solid surface:

$$\Delta T_G = T_{Ge} - T_{Gf}. \tag{5}$$

With the mass m_G of the gas involved and its heat capacity c_G the exchanged heat energy Q_G can be calculated as

$$Q_G = m_G \Delta T_G c_G. \tag{6}$$

The above assumption that heat energy, causing the thermal anomaly, is provided (or absorbed) solely by the gas through conduction, leads to

$$Q_G = \Delta Q_R, \tag{7}$$

and to the elapsed mass of gas involved

$$m_G = \frac{\int_t \int_A | E_n - E_a | \, \mathrm{d}A \mathrm{d}t}{\Delta T_G c_G}. \tag{8}$$

To apply Eq. (8), several parameters are to be known, namely the temperatures T_a, T_n, T_{Ge} and T_{Gf}, the area of thermal reach A and the time of observation t.

3. RESULTS AND DISCUSSION

3.1. Gas vents at the Bossoleto doline

The doline Bossoleto is located on the eastern master fault of the Siena Graben (Tuskany, Italy), known as Rapolano fault. It was selected as natural vent of large amounts of carbon dioxide CO_2 from the prevailing deep geothermal reservoirs. It appears as a nearly circular bowl-like depression of top diameter about 80 m and of the ground diameter 40–50 m at the depth of 6 m. The edge and partly the slopes are covered by trees whereas reed grows on much of the flat bottom which also contains extended areas of bare dark soil and regions of travertine rubble. A stone wall of about 2.5 m height around the doline and a lockable door prevent unwanted admission since the site presents peril to life of humans and animals.

For investigations, in addition to the AGEMA 570 thermovision camera, a CO_2 probe of the type "Deponiegasmonitor Ansyco 2000" was employed. Via a plastic hose the instrument aspirates air/gas into its measurement compartment and determines CO_2 concentration applying optical absorption techniques. With the aid of this instrument several gas exits were detected by systematic search at half buried smaller and larger rocks at various locations of the bottom and the transition to the slopes of the doline (Figs. 1, 2).

The site is at the transition of the bottom to the northern slope of the doline covered by travertine rubble. It is shown in Fig. 1 with the test area marked red. Two vents were found, their location is marked by red circles in Fig. 1.

In all cases CO_2 concentrations higher than 95% were measured directly at the vent outlet. A test area was selected based on the gas vents found.

3.2. Measurement

To acquire thermal images of the test area, an AGEMA 570 camera was attached to the top of an aluminium ladder, positioned on a plateau at half height of the slope opposite to the test area. The distance between the camera and the centre of the test area was 48 m.

Time sequence of the thermal image of the test area was recorded starting at 16:57 on May 16th and ending at 09:21 on May 17th, 2005. It contains 985 congruent frames taken at one minute intervals for an area of approximately 10 m wide and 7.5 m high. Each camera pixel corresponds to a square oxel of approximately 3.1 cm side length. The infrared image time series provides information on the oxel surface radiance temperature T_S as a function of time t

and location given by the pixel coordinates x and y, which correspond to appropriate oxel coordinates in the scene

$$T_S = f(t, x, y). \tag{9}$$

3.3. Detection of vents

The minimal thermal change detection operation was applied to 200 images taken between 17:46 and 21:06. The result of this process is the image frame of maximum temperature differences (Fig. 3) according to Section 2.3. Three thresholds have been set and marked by blue colour for the region of lowest difference of 4 to 7°C, green colour for 7 to 9°C, where the gas exits are located and red colour for 9 to 10°C, the latter under thermal influence of the gas. The dark grey area is free of vents, temperature differences being above 10°C. Obviously there are more than the two vents that have been detected with the CO_2 probe, the smaller ones of which would be difficult to find with conventional methods. The vents are concentrated to a travertine rubble area of approximately 5×2.8 m within the lower end of the depression slope extending down to the depression bottom. More vents are obviously above the travertine rubble between bushes and treetops at the doline's slope.

3.4. Gas quantity

As stated above, temperatures T_a, T_n, T_{Ge} and T_{Gf}, as well as the area of thermal reach A and the time duration t of heat exchange need to be determined.

3.4.1. Exit temperature T_{Ge} of the vent gas

The observed gas exits are located on slopes where the "heavy" CO_2 flows downhill leaving a thermal trace. Along the slope of the most important exit the temperature over time has been investigated in detail by extracting the temperature course of 19 distinctive neighbouring spots on congeneric ground, numbered along descending temperature and each containing a few pixels (Fig. 4).

The spot of lowest temperature change is identified as the gas exit. The temperature course of this spot AR01 and of two other spots, AR10 in the middle and AR19 at the end of the selected part of the slope, are shown in Fig. 5.

Figure 5 reveals a "crossover" of temperature courses between about 18:37 and 18:40. Prior to crossover, when the scene is sunlit, the gas exit spot AR01 is cooler than the spots AR10 and AR19, because the emerging gas cools the spot. After crossover, the exit spot, being warmed by the gas, has a higher temperature than its vicinity, which, not sunlit any more, cools down. The exit spot AR01 itself undergoes the least temperature change over time and the most distant spot AR19 the highest. The crossover temperature of about 19°C resembles the gas exit temperature T_{Ge}, thus the vent gas temperature. Besides, the diagram demonstrates the characteristics of minimal thermal exchange.

3.4.2. Thermal reach and final temperature T_{Gf} of the vent gas

After finalization of the heat energy exchange, temperatures of the surface and gas are assumed to be the same, denoted by T_{Gf}. Starting at the vent itself, the temperature gradient to consecutive neighbouring pixels is determined proceeding along the thermal trace until it becomes zero. The area beyond is not influenced by the gas and hence has homogeneous temperature. Its temperature is T_{Gf} and in this way also the area of thermal reach A and its coordinates are determined. Furthermore, T_{Gf} equals T_n. The remaining parameter to be determined is the temperature of the thermal anomaly T_a, which can be taken from appropriate pixels of every image frame with the knowledge of the thermal reach area A coordinates. Figures 6 and 7 illustrate the method. The temperature courses at AR03 and AR04 are the same, but different from courses at AR01 and AR02, which are closer to the vent and are influenced by the gas. Areas AR03 and AR04 are out of the thermal reach of the gas. Temperature crossover occurs at about 21:30 prior to which areas AR01 and AR02 are cooled by the gas and after which they are warmed.

As can be seen from Fig. 7, the area of thermal reach changes with time since the ambient (non-gas) thermal influence is a function of weather. To the contrary, the gas flow is considered constant over time and thus the gas heat energy flux is constant, too. Hence the constant gas heat flux provides thermal compensation for varying ambient energy flux.

3.4.3. Amount of the emitted gas

Above survey of acquired data reveals that not all of the gas vents of the test area are congeneric. Especially the vent at the upper left side is between bushes and treetops, whereas the lower ones are on travertine rubble (Figs. 1 and 3). Yet, the method described is expected to be applied to congeneric areas. Furthermore, it requires optical access to the areas surrounding the vents in order to determine the thermal reach area A. This is not the case for the considered vent; the vegetation obstructs the view to the surrounding ground and constrains the thermal reach determination. In order to account for this, gas flow calculations have been applied to a vent area, restricted to the travertine rubble and its close vicinity, represented by the frame pixels ranging from 50 to 140 on the vertical axis and from 160 to 260 on the horizontal axis (Fig. 3).

The time period between 19:00 and 23:10 shows a steady thermal course, the scene is out of the sun for quite a while and temperatures were decreasing. Emitted gas quantity has been determined from the data acquired within this time period consisting of 250 frames. Since there was no means to measure the spectral emissivity of the surface material (travertine rubble), the value of emissivity was estimated to be 0.8 for the calculations of the radiation flux E with reference to Eqs. (1) and (2). Table 2 shows the results.

Table 2. Gas flow parameters in the travertine rubble area, derived from data taken from 19:00 to 23:10 (frame step 1 min.)

Area of thermal reach, m^2	2.4
Gas flow, litre/min	8.8
Gas quantity, tons/day	0.025
tons/year	9
Doline extrapolated quantity, tons/year	3400

Furthermore, an extrapolated total doline emitted gas quantity has been calculated based on the assumption that vents in the spatial average are equally spread all over the doline surface. Thus this value is referenced to the ratio of total doline surface area to image area. Interestingly, the resulting quantity of 3400 tons/year (Table 2) is very close to the cited estimation of 3500 tons/year in [1]. However, it must be mentioned that neither the assumption of equally spread vents has been proven nor can the surface area calculation be considered as highly accurate. This is due to the fact that by far not all vents are known and that surface topography data of the doline are not available. The calculations assume an ideal frustrum surface. Also the observation geometry was approximated to be a plane surface perpendicular to the line of sight of the camera. Also here considering topography data would enhance accurarcy. Nevertheless, the matching of [1] with this work can be considered as an indication that the order of magnitude of the achieved result is correct, at least.

Figure 8 shows the image of maximum thermal differences, those of least differences in blue (vents) and green, whereas red marks the spots resembling the temperature after finalization of thermal energy exchange T_{Gf}. The blue and green region thus depicts the area of thermal reach of the gas.

4. CONCLUSIONS

It has been proven that minimum thermal exchange detection is appropriate to discover unknown vents of CO_2 in suspect terrain from time series of infrared images. Vent gas temperature can be derived as well as the area of thermal influence of the gas on the terrain. A method has been developed to derive gas flux quantities from such data. Gas amount can be extrapolated to the neighbouring terrain. It is remarkable that besides thermal images no other data are required. Taking into account the complexity of the investigated events, intensive research on the new method is still on the way and the results presented here have to be considered as preliminary with respect to quantitative conclusions.

Being a remote sensing method, it could be applied to airborne and spaceborne measurements. Since thermal anomalies may be caused not only by emerging gas, other applications are worth to be developed such as detection and quantification of coal seam fires, soil moisture reservoirs, cold/warm water bodies, etc.

Fig. 1. Vent under a small rock in travertine rubble; the dry grass (agrostis canina) on the right allows estimation of the size of the vent.

Fig. 2. Photo of the interior of the Bossoleto depression, test area and location of two small vents marked red.

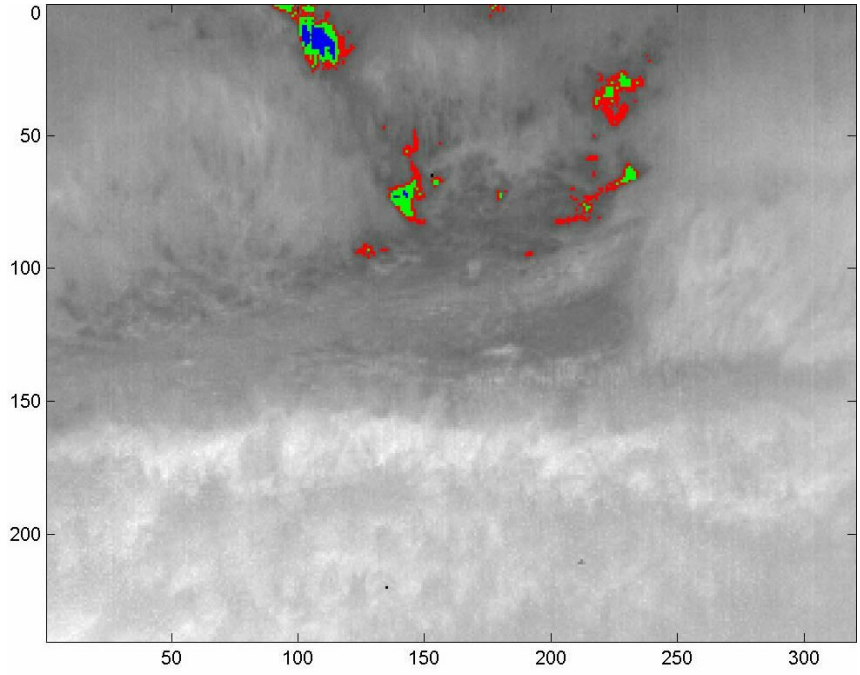

Fig. 3. Map of vents, detected within the test area (marked by red frame in Fig. 1); the colours show temperature differences, blue for 4 to 7 °C, green for 7 to 9 °C, red for 9 to 10 °C and dark grey for above 10 °C.

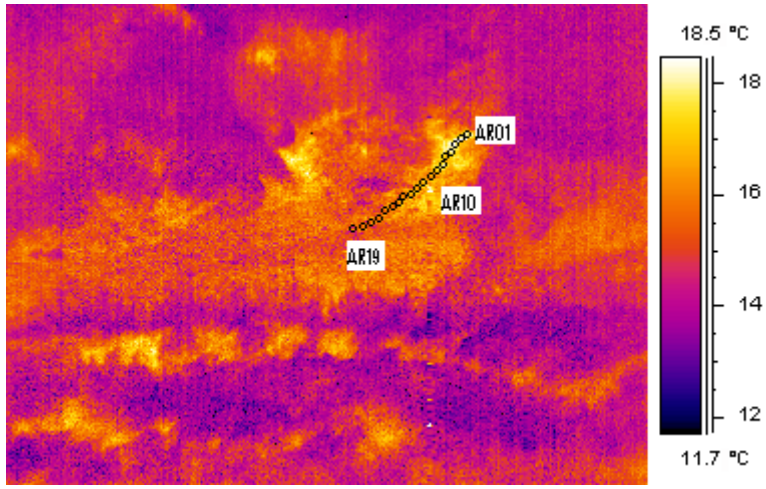

Fig. 4. Thermal image with 19 small areas marked along the thermal trace of the vent. The areas are the lower row of small circles. Above this row of circles is the numbering AR01 to AR19 from right to left. Unfortunately, beyond our control inscription is mostly overlapping and hence illegible.

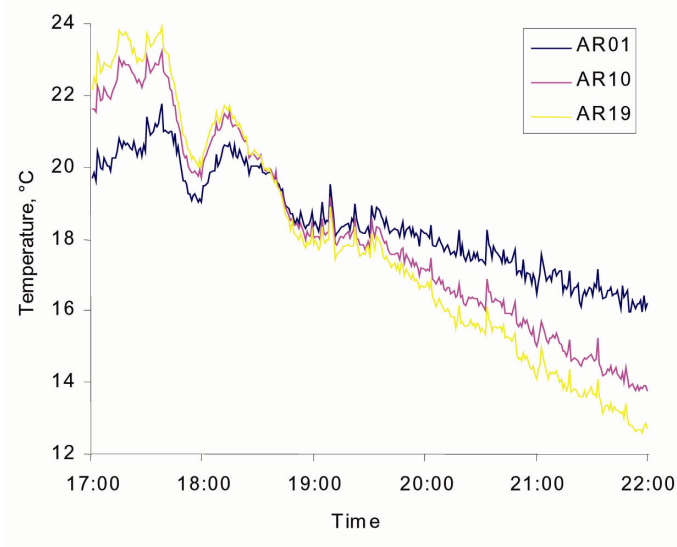

Fig. 5. Temperature course of selected small areas in thermal reach of the most important vent, shown in Fig. 4; crossover temperature was about 19 °C at around 18:40.

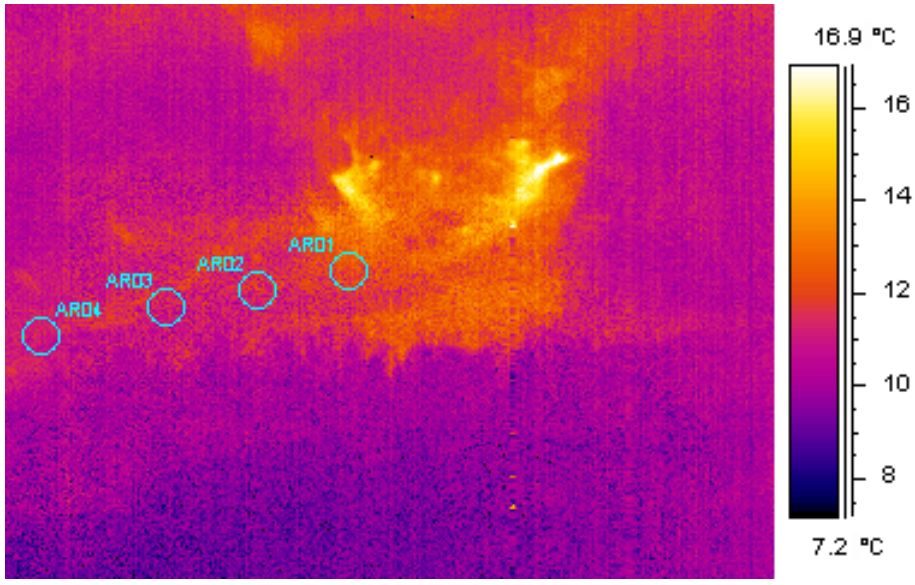

Fig. 6. Thermal image and marked congeneric areas along the thermal trace chosen to determine the thermal reach.

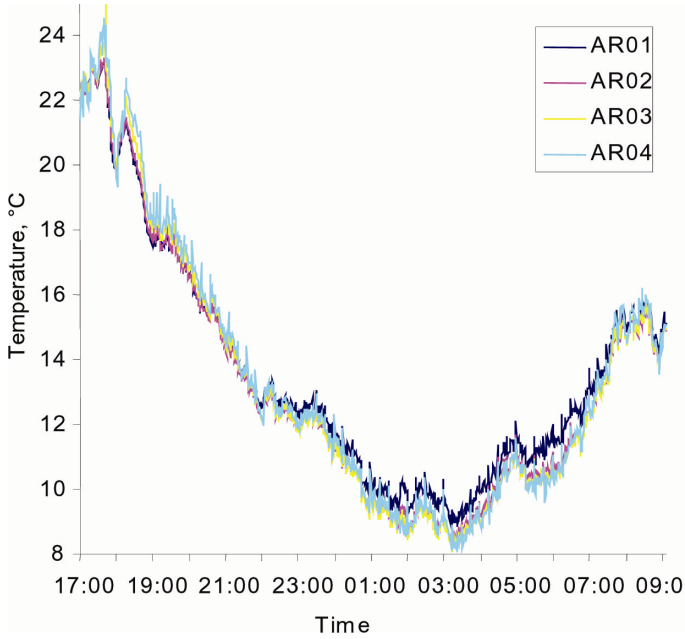

Fig. 7. Temperature course of selected areas shown in Fig. 6.

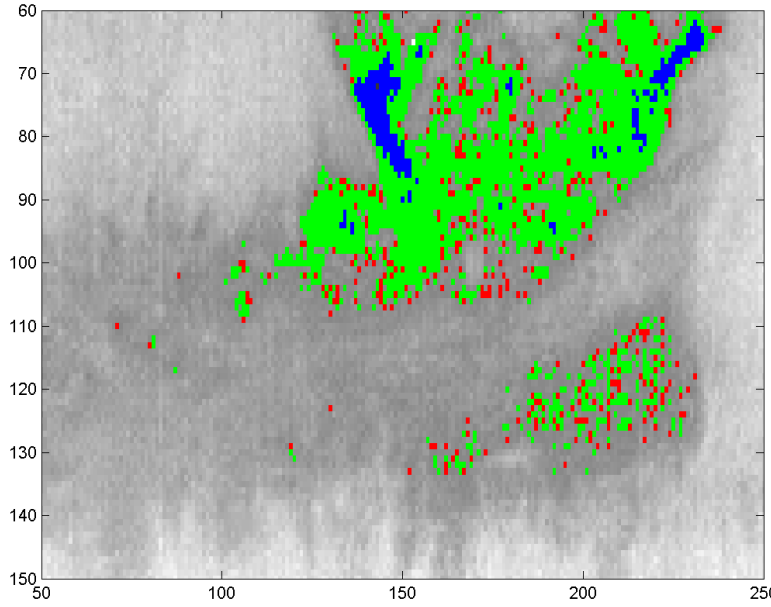

Fig. 8. Maximum temperature differences between 19:00 and 23:10; blue – vents; green – thermal reach area; red – no gas influence reference area; grey – out of gas influence. Image restricted to the travertine rubble vent area and its close vicinity, pixel numbers on axes allow orientation in comparison to the total scene (Fig. 3).

ACKNOWLEDGEMENTS

The author is grateful to E. and P. Bankwitz, H. Kämpf, H. Pfanz and D. Vodnik for many helpful discussions, which laid the ground for the development of the methods described. He thanks A. Raschi and H. Pfanz for providing logistic support for the field experiments at Bossoleto.

REFERENCES

1. Mörner, N.-A. and Etiope, G. Carbon degassing from the lithosphere. *Global and Planetary Change*, 2002, **33**, 185–203.
2. Raschi, A., Vaccari, F., Tognetti, R. and van Gardingen, P. R. (eds.). *Plant Response to Elevated CO_2*. Cambridge University Press, Cambridge, 1997.
3. Vodnik, D., Pfanz, H., Wittmann, C., Maček, I., Kastelec, D., Turk, B. and Batič, F. Photosynthetic acclimation in plants growing near a carbon dioxide spring. *Phyton*, 2002, **42**, 239–244.
4. Pfanz, H., Vodnik, D., Wittmann, Ch., Aschan, G. and Raschi, A. Plants and geothermal CO_2 exhalations – survival and adaptation to a high CO_2 environment. In *Progr. Botany*, 2004, **65**, 499–538.
5. Weinlich, F. H., Tesař, J., Weise, S. M., Bräuer, K. and Kämpf, H. Gas flux distribution in mineral springs and tectonic structure in the western Eger Rift. *J. Czech. Geol. Soc.*, 1998, **43**, 1–2.
6. Tank, V. Verfahren zum Feststellen von Gasaustritten an der Erdoberfläche und Anordnung zu dessen Durchführung. European Patent 04 787 022.5, filed 2003, issued 2007.

Minimaalsete soojusmuutuste detekteerimisel põhinev uut tüüpi instrument termiliste anomaaliate kaugmõõtmiseks

Volker Tank

Termilised anomaaliad on ettenägematud kõrvalekalded normaalsetest soojuslikest käitumistest, mille taga võivad peituda olulised mittesoojusliku päritoluga nähtused, näiteks gaaside väljapääs sügavatest reservuaaridest läbi maakoore või allikavee. Artiklis on käsitletud uut meetodit loodusliku süsihappegaasi väljapääsukohtade avastamiseks termiliste kõrvalekallete kaudu, samuti instrumente selle meetodi rakendamiseks.